International Journal of Electrical, Electronic and Communication Sciences
ISSN: 2517-9438
Vol:5, No:10, 2011

Characterization and Modeling of Piezoelectric Integrated Micro Speakers for Audio Acoustic Actuation

J. Mendoza-López, S. Sánchez-Solano, J. L. Huertas-Díaz

***Abstract*—**An array of piezoelectric micro actuators can be used for radiation of an ultrasonic carrier signal modulated in amplitude with an acoustic signal, which yields audio frequency applications as the air acts as a self-demodulating medium. This application is known as the parametric array. We propose a parametric array with array elements based on existing piezoelectric micro ultrasonic transducer (pMUT) design techniques. In order to reach enough acoustic output power at a desired operating frequency, a proper ratio between number of array elements and array size needs to be used, with an array total area of the order of one cm square. The transducers presented are characterized via impedance, admittance, noise figure, transducer gain and frequency responses.

***Keywords*—**Pizeoelectric, Microspeaker, MEMS, pMUT, Parametric Array

I. Introduction

MULTIMEDIA systems and components such as micro speakers are key elements for the needs of mobile phone, entertainment and computer industries, but also of increasing interest for aerospace applications. The term "micro speaker" is however a contradiction in itself: "micro" denotes microscopic and as such only microscopic wavelengths or, equivalently, ultrasonic frequencies can be processed. Micro actuators operate in the ultrasonic frequency range due to their microscopic size and therefore can only radiate small wavelengths, far beyond the human hearing capability. A promising possibility to have micro actuators ultimately produce acoustic signals is the parametric array [1].

Parametric array applications and performance in air have long been studied since its initial proposal by Westervelt [2], and applications and design of the parametric array in water have also been discussed [3-7]. The idea is to have the array radiate an ultrasonic carrier signal modulated in amplitude with an acoustic signal. Due to the nonlinear nature of the air, its behavior as a self-demodulator results in a highly directive audio beam. Possible applications include the acoustic torch or audio spotlight [8, 9].

The main problem of the parametric array in air has been reported as its highly distorted acoustic output, measured by total harmonic distortion [10], for which some possible improvements such as preprocessing techniques [11, 12], or psycho acoustic masking [13] have been proposed. Different amplitude modulation strategies such as single side band amplitude modulation, double side band amplitude modulation or square root amplitude modulation, amongst others, have been tried in the past [14].Wygant et. al. [15, 16] proposed a parametric array made of capacitive micro ultrasonic transducers (cMUTs), which are simpler to fabricate with well-established MEMS foundry technologies than their counter piezoelectric analogues (pMUTs), as they require just an electrostatically actuated moving polysilicon membrane. The original idea of such a cMUT parametric array was speech transmission over large distances. For a 5 kHz acoustic input signal they achieved an output acoustic pressure level of 58 dB at 3 m distance, with a beam width of less than 10 degrees. However, some works [17, 18] have claimed pMUTs to have a superior performance in terms of efficiency and signal-to-noise ratio due to the exceptional properties of synthetic materials such as PZT.

In this paper a parametric array composed of piezoelectric micro ultrasonic transducers (pMUTs) is proposed in order to ultimately achieve a highly directional audio beam and a high efficiency, without the need of high bias voltages and parasitic capacitances imposed by the very nature of the cMUTs. We present a thorough electromechanical characterization of the pMUT transducers intended to make up the parametric array including noise figures, frequency responses, impedance, admittance and transducer gain.

II. Transducers

The transducers presented consist of square piezoelectric unimorphs with a silicon substrate followed by a Si3N4 - PolySi – Au – PZT – Au layer stack, as shown in Fig 1, in thickness mode excitation. The square geometry was chosen for the added easiness provided in stacking several micro transducers for large arrays. Their resonance frequency vs. size relationship was obtained as inversely proportional to one another.

In order for the secondary beam to reproduce audio frequencies, the difference between the carrier frequency, f_c, and the message frequency, f_m, has to be contained in the

J. M. L. is with the Institute of Microelectronics of Seville (IMSE), Spanish National Centre of Microelectronics (CNM), 41092 Sevilla, Spain (phone: +34 954466613; fax: +34 954466600; e-mail: mendoza@imse-cnm.csic.es).

S. S. S. is with the Institute of Microelectronics of Seville (IMSE), Spanish National Centre of Microelectronics (CNM), 41092 Sevilla, Spain (phone: +34 954466623; fax: +34 954466600; e-mail: santiago@imse-cnm.csic.es).

J. L. H. D. is with the Institute of Microelectronics of Seville (IMSE), Spanish National Centre of Microelectronics (CNM), 41092 Sevilla, Spain (phone: +34 954466656; fax: +34 954466600; e-mail: huertas@imse-cnm.csic.es).

This work has been partially supported by the E.S.A. project COSMIC VISION.

audio range i.e. no more than 20 kHz: For a carrier frequency of 25 kHz, a message signal of 15 kHz would produce a secondary wave component at 10 kHz.

For transducers not to be too large we can choose a transducer side length of 5 mm which would mean an operating frequency of 632 k. This way a wave at 637 kHz would be demodulated at 5 kHz, well in the audible range.

The described devices are intended to be fabricated by stacking electroded layers of piezoelectric material on a silicon membrane on a substrate, followed by an etching on the back side of the substrate to release the moving membrane. The design parameter ranges are specified in Table I.

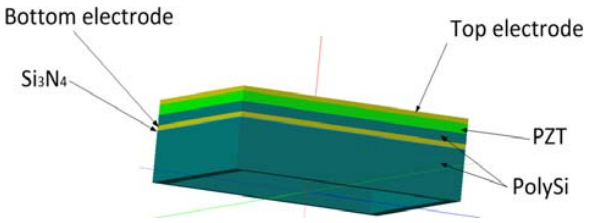

Fig. 1 Schematic cross sectional view of simulated actuator. Layers, from top to bottom: top electrode, piezoelectric layer(s), bottom electrode, nitride layer, polysilicon structural layer

III. Theoretical Background

A. Acoustic Propagation

Acoustic propagation in nonlinear media can be described by the well-known Khokhlov–Zabolotskaya–Kuznetsov (KZK) nonlinear parabolic wave equation [19]:

$$\frac{\partial p}{\partial z}=\frac{c_0}{2}\int_{-\infty}^{\tau}\left(\frac{\partial^2 p}{\partial \tau^2}+\frac{1}{r}\frac{\partial p}{\partial r}\right)d\tau'+\frac{\beta p}{\rho_0 c_0^3}\frac{\partial p}{\partial \tau}+\frac{\delta}{2c_0^3}\frac{\partial^2 p}{\partial \tau^2}+\sum_{\upsilon}\frac{c_\upsilon'}{c_0^2}\int_{-\infty}^{\tau}\left(\frac{\partial^2 p}{\partial \tau'^2}e^{-(\tau-\tau')/t_\upsilon}d\tau'\right) \quad (1)$$

where p = p(r,z,t) is the sound pressure, ρ_0 and c_0 are the air density and speed of sound respectively, z is the on-axis beam propagation direction coordinate, t is the time, δ stands for the dissipation factor of thermoviscous absorption, τ = t – z/c0 is the retarded time, tυ is the relaxation time that characterizes each relaxation process υ (being υ a positive integer), and c_υ' represents a small-signal sound speed increment.

The four terms on the right-hand side of (1) account for diffraction, nonlinearity, thermoviscous absorption, and relaxation effect, respectively. The KZK equation can be solved numerically after applying a coordinate transformation and integrating each term separately at sufficiently small steps in the time domain [20] or following other techniques in the frequency domain [21].

B. Piezoelectric Actuation

Following the IEEE Standard on Piezoelectricity [22], the linear piezoelectric constitutive equations relating the electrical field $E_{i=1\text{-}3}$ in the case of actuators or the spatial polarization vector $P_{i=1\text{-}3}$ in the case of sensors to the corresponding longitudinal and shear components of the mechanical stress $T_{j=1\text{-}6}$ or strain $S_{j=1\text{-}6}$ tensors are:

TABLE I
Transducer Design Variables (μM)

Meaning	Symbol	Min. value	Max. value
Sustrate thickness	t_{sus}	400	1000
PolySi thcikness	t_{Poly}	0.5	10
Si_3N_4 thickness	t_{Si3N4}	0.5	10
Electrode thickness	t_{el}	0.5	10
PZT thickness	t_{PZE}	0.5	25
Side length	L	1k	100k

$$\boldsymbol{S}_{j=1-6}=\sum_{i=1}^{3}\boldsymbol{d}_{ij}\boldsymbol{E}_{i=1-3}+\sum_{h=1}^{6}\left(1/\boldsymbol{C}_{jh}^{E=cte}\right)\boldsymbol{T}_j \quad (2)$$

$$\boldsymbol{T}_{j=1-6}=-\sum_{i=1}^{3}\boldsymbol{e}_{ij}\boldsymbol{E}_{i=1-3}+\sum_{h=1}^{6}\boldsymbol{C}_{jh}^{E=cte}\boldsymbol{S}_j \quad (3)$$

where $\boldsymbol{d}_{ij}$ [m/V] and $\boldsymbol{e}_{ij}$ [C/m^2] are the piezoelectric 3x6 constants of the piezoelectric material, and the indexes *i* and *j* denote polarization and actuation direction, respectively. $\boldsymbol{C}_{jh}$ represents the 6x6 elastic stiffness of the piezoelectric material under constant electric field, and it relates the two piezoelectric constant types following the expression:

$$\boldsymbol{e}_{mh=1-6}=\sum_{h=1}^{6}\boldsymbol{C}_{jh}^{E=cte}\boldsymbol{d}_{mj} \quad (4)$$

The dielectric polarization $P_{i=1\text{-}3}$ of the piezoelectric material is expressed as:

$$\boldsymbol{P}_{i=1-3}=\boldsymbol{D}_{i=1-3}-\varepsilon_0\boldsymbol{E}_{i=1-3}=\sum_{k=1}^{3}(\varepsilon_{ij}-\varepsilon_0)\boldsymbol{E}_{i=1-3}+\sum_{j=1}^{6}\boldsymbol{e}_{ij}\boldsymbol{S}_{j=1-6} \quad (5)$$

with ε_{ij} (units of F/m) and D_i (units of C/m^2) represent the 3x3 permittivity matrix and electric displacement vector, respectively, and ε_0 is the permittivity of free space. Eqns. (2) to (5) are the existing fundamental piezoelectric constitutive equations which describe the membrane behavior.

C. Transducer as a Two-Port Network

For the electromechanical analysis of our interest, a piezoelectric actuator can be described as a linear two-port network (Fig 2), for which the following relations hold between electrical and mechanical inputs and outputs for harmonic excitation under standard electromechanical analogy:

$$\begin{bmatrix}\boldsymbol{F}\\-\boldsymbol{u}\end{bmatrix}\equiv\begin{bmatrix}\boldsymbol{V}_o\\\boldsymbol{I}_o\end{bmatrix}=\begin{bmatrix}Z_{11}&Z_{12}\\Z_{21}&Z_{22}\end{bmatrix}\cdot\begin{bmatrix}\boldsymbol{V}_i\\\boldsymbol{I}_i\end{bmatrix} \quad (6)$$

where V and I denote complex voltage and current and the subscripts i and o denote input and output, respectively. F and u denote complex force and particle velocity on the front face of the transducer, and the matrix Z containing elements Z_{11}, Z_{12}, Z_{21}, and Z_{22} is the complex impedance matrix for the transducer viewed as a two-port network. By modelling the transducer with a numerical simulation environment such as SPICE or Spectre, data for the impedance matrix or particle velocity amongst other quantities can be obtained. For a more detailed analytical two-port, lumped-element modelling of a piezoelectric unimorph composite circular plate see [23]. In our work, the matrix Z was computed with Spectre after modelling the actuator with a commercial MEMS prototyping and design software.

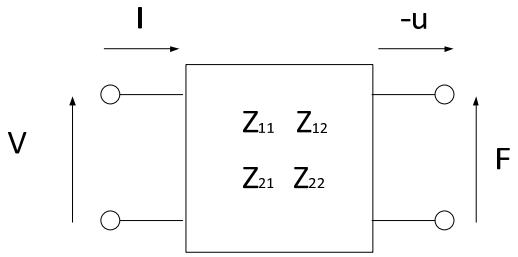

Fig. 2 The electromechanical transducer represented schematically as a two-port network

D. Vibration Problem

In order to relate the acoustics of the device to the intrinsic material properties of the membrane, the problem has to be tackled from an electro-mechano-acoustical perspective. In the mechanical domain considering vibrating plates, Euler's flexural equation of motion for a forced circular plate with clamped edges would apply. According to our results and following previous work on vibrating piezoelectric circular diaphragms [24], piezoelectric micromachined devices behave more like membranes (resonance frequencies proportional to L^{-1}) than like thin plates (resonance frequencies proportional to L^{-2}). Therefore the problem can be formulated as a forced circular membrane with clamped edges, for which the equation of motion is:

$$T\nabla^2 w(\mathbf{r},t) + \rho_0 \frac{\partial^2 w(\mathbf{r},t)}{\partial t^2} = f(\mathbf{r},t) \quad (7)$$

where $w(\mathbf{r},t)$ is the membrane's displacement at a point pointed by vector $\mathbf{r}$ at an instant t, $f(r,t)$ is the forcing function at any point pointed by $\mathbf{r}$ at an instant t, T is the tension on the membrane, ∇^2 is the Laplacian operator and ρ_0 is the material density. Solving eqn. (7) for $w(\mathbf{r},t)$ with the appropriate boundary conditions corresponding to clamped edges gives an expression for the displacement at any point of the membrane at any instant t, given a known forcing function. The solution to eqn. (7) is usually not easy to compute and analytical solutions might not exist depending on the geometry and boundary conditions. Finite integral transforms might be obtained [25] or alternatively numerical solutions can be computed by the finite element and boundary element methods [26].

IV. Results

The commercial software MEMS+™ from Coventor Inc. was used for transducer design and visualization in conjunction with Cadence Virtuoso™ as a numerical calculation engine. An AC analysis was performed to calculate the frequency response voltages and currents. An s-parameter analysis was used for impedance, admittance, noise figure and transducer gain calculation. Both analyses were computed between 1kHz and 10 MHz.

As it can be seen in Fig 3 impedance magnitude goes down and impedance resonance frequencies lower as side lengths increase. Admittance behavior is obviously the opposite: magnitude goes up and resonance frequencies also go down in the same fashion as side lengths increase (Fig 4). To illustrate how resonance frequencies change as a function of side length or piezoelectric layer thickness the values of the resonance peaks can be plotted for each length or thickness, extending the data presented in Fig 5 and Fig 6 to that shown in Fig 3 and Fig 4, where lengths ranged 1 to 10 mm and thicknesses ranged 0.5 to 25 μm.

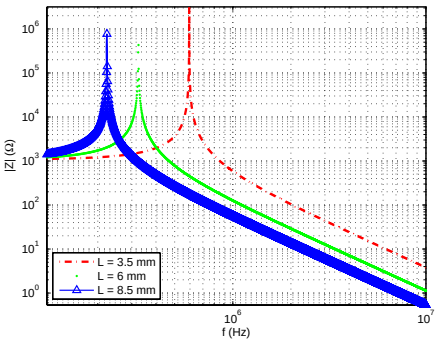

Fig. 3 Transducer impedance magnitudes calculated for different side lengths, all of them for a piezoelectric layer thickness of 0.5 μm

Plotting the data of Fig 5 against inverse length, a straight line was found. This means that the transducer first resonance frequency is inversely proportional to the length, corroborating the findings of [24] which mean that these diaphragms would behave as membranes rather than as thin plates.

Three sample transducer frequency responses for side lengths of 2.4, 2.9 and 8.4 mm and piezoelectric thicknesses of 4, 5 and 6 μm are shown in Fig 7 and Fig 8, respectively.

Depending on the values of transducer side lengths or piezoelectric thicknesses, the resonance peaks in transducer frequency response magnitude might increase more or less with respect to each other. To have a complete picture of how lengths and thicknesses affect the impedance or transducer frequency response peaks, 3D plots are presented in Fig 9 to Fig 12 at different fixed frequencies.

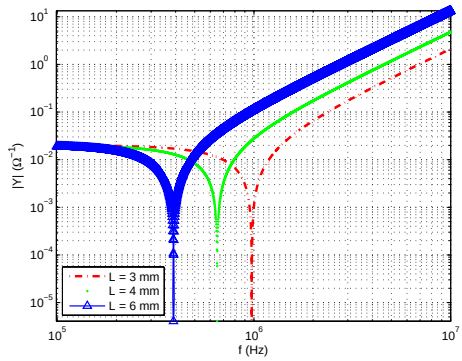

Fig. 4 Transducer admittance magnitudes calculated for different side lengths, all of them for a piezoelectric layer thickness of 0.5 µm.

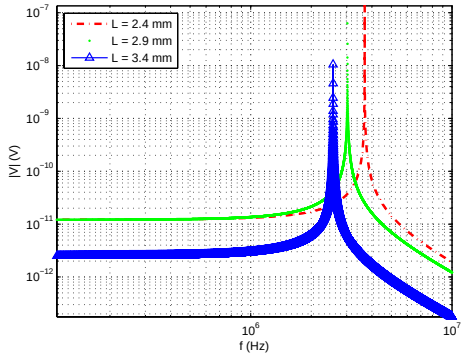

Fig. 7 Transducer electromechanical frequency response magnitudes for different side lengths

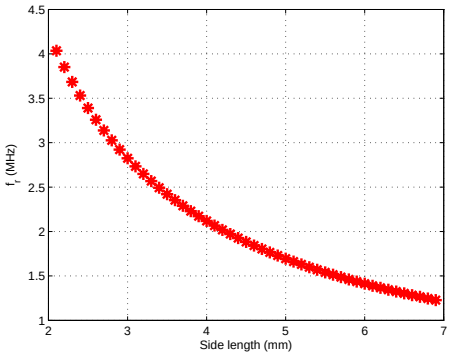

Fig. 5 Resonance frequency versus transducer side length calculated for a piezoelectric layer thickness of 1 um

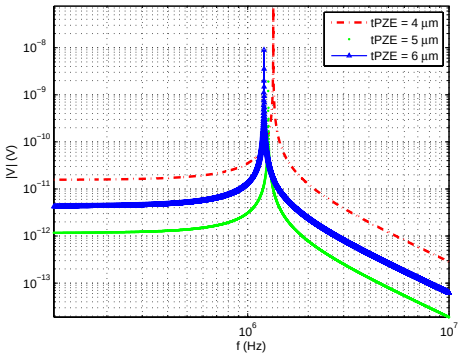

Fig. 8 Transducer electromechanical frequency response magnitudes for different piezoelectric layer thicknesses

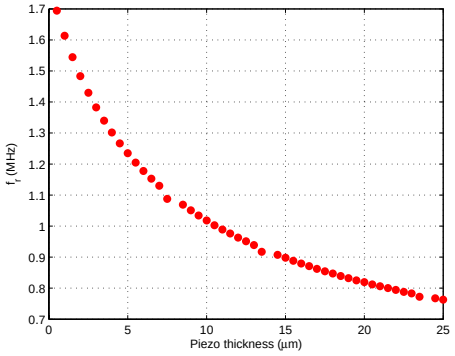

Fig. 6 Resonance frequency versus piezoelectric thickness calculated for a side length of 5 mm

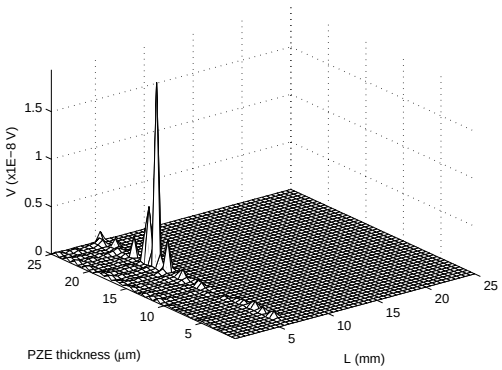

Fig. 9 Resonance frequencies versus side length and piezoelectric thickness at a frequency of 0.5 MHz

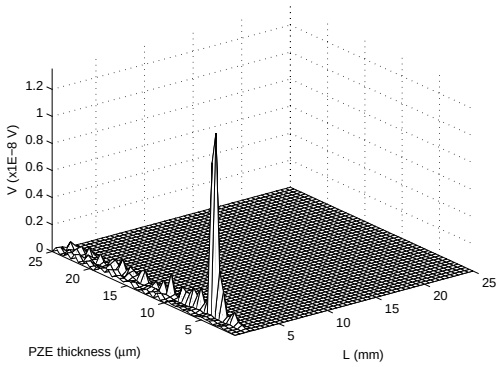

Fig. 10 Resonance frequencies versus side length and piezoelectric thickness at a frequency of 1.5 MHz

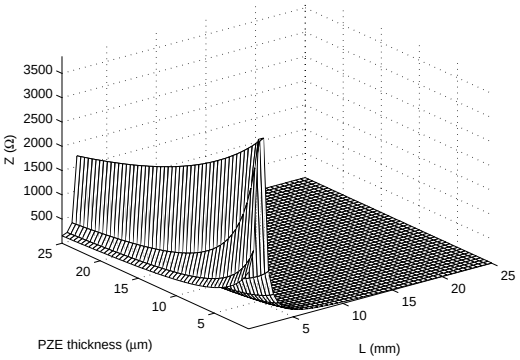

Fig. 11 Impedance peak values versus side length and piezoelectric thickness at a frequency of 1 MHz

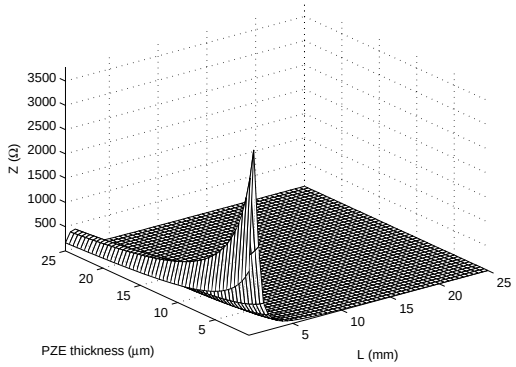

Fig. 12 Impedance peak values versus side length and piezoelectric thickness at a frequency of 1.5 MHz

As frequency increases, impedance peak values tend to decrease faster with increasing piezoelectric layer thickness (Fig 11 and Fig 12), and frequency response peak values tend to concentrate around a region with lower side length and piezoelectric layer thickness (Fig 9 and Fig 10). Noise figure and transducer gain are characterized in a similar manner: the values of either NF versus side length or NF versus piezoelectric layer thickness can be plotted for a given frequency range (Fig 13 and Fig 14), and similar plots can be obtained for transducer gain (Fig 15 and Fig 16).

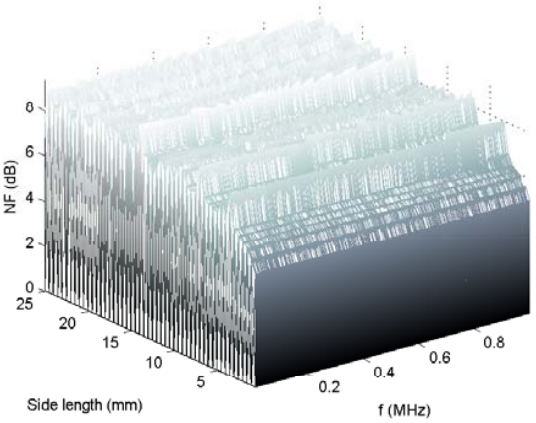

Fig. 13 Noise figure versus side length up to frequencies of 2 MHz, for a fixed piezoelectric layer thickness of 5 μm

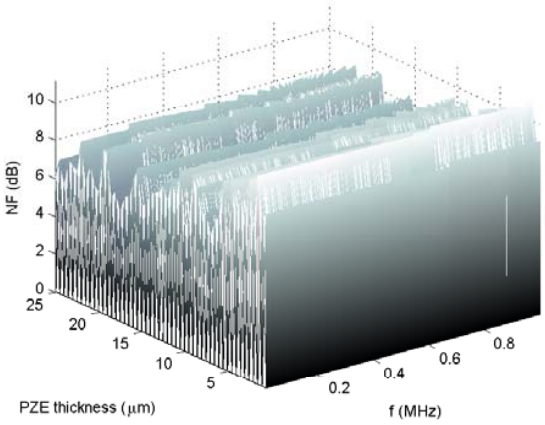

Fig 14 Noise figure versus piezoelectric layer thickness up to frequencies of 2 MHz, for a fixed side length of 3 mm

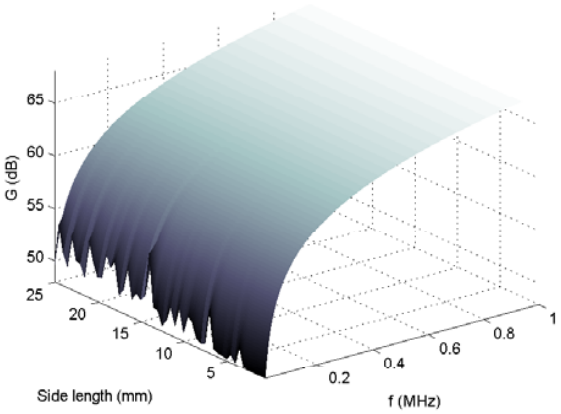

Fig. 15 Transducer gain versus side length up to frequencies of 2 MHz, for a fixed piezoelectric layer thickness of 5 μm

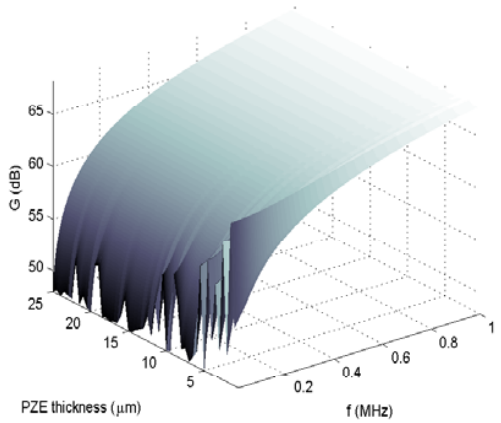

Fig. 16 Transducer gain versus piezoelectric layer thickness up to frequencies of 2 MHz, for a fixed side length of 3 mm

V. Discussion

The results presented characterize the transducer design space and yield information and details on impedance, resonance frequency, noise figure and transducer gain as a function of frequency, piezoelectric layer thickness and transducer side length.

The main variables considered in this study induce to treat the problem as a 4-variable problem: frequency (f), piezoelectric layer thickness (t_{PZE}), side length (L) and one other variable for the z-axis which can be either frequency response (V), impedance (Z), admittance (Y), noise figure (NF) or transducer gain (G).

Therefore, 3D plots can be made of any of the z-axis variables with respect to two other independent variables after fixing the remaining one. For example, a 3D plot can be obtained of $|Z|$ versus piezoelectric thickness and transducer side length at any fixed frequency. Similarly, if transducer side length was fixed, the plot of $|Z|$ versus piezoelectric thickness and frequency could be produced. Alternatively, two variables might be fixed and the remaining two can be plotted against each other, which yield a plot matrix. This approach introduces a complete way of characterization of the piezoelectric transducer based on an sp-analysis. Any two independent variable values might be set and the relation with the two others might be obtained numerically.

VI. Conclusion

The main design parameters and analysis of square pMUTs is presented for audio application in a parametric array. The transducer analysis, based on s-parameter analysis for a two-port network, yielded values for impedance, admittance, frequency response, noise figure and transducer gain. Relationships between transducer side length, piezoelectric layer thickness and operating frequency have been presented and constitute a useful trade-off towards the optimal performance of a parametric array based on such piezoelectric transducers.

Acknowledgments

J.M.L. Author thanks partial funding by the postdoctoral program JAE-DOC granted by the Spanish National Research Council (Consejo Superior de Investigaciones Científicas C.S.I.C.)

References

[1] M. F. Hamilton, "Audio parametric arrays in air," The Journal of the Acoustical Society of America, vol. 125, pp. 2688-2688, 2009.
[2] P. J. Westervelt, "Parametric acoustic array," Journal of The Acoustical Society of America, vol. 35, pp. 535-&, 1963 1963.
[3] W. S. Liu and Z. X. Xu, "Propagation of the difference frequency wave generated by a truncated parametric array through a water sediment interface," Journal of The Acoustical Society of America, vol. 89, pp. 92-97, Jan 1991.
[4] K. L. Williams, L. J. Satkowiak, and D. R. Bugler, "Linear and parametric array transmission across water-sand interface - Theory, experiment and observation of beam displacement," Journal of The Acoustical Society of America, vol. 86, pp. 311-325, Jul 1989.
[5] J. M. Huckabay, "An experimental study of parametric acoustic arrays with intermediate directivity in water," Journal of The Acoustical Society of America, vol. 67, pp. 1480-1485, 1980 1980.
[6] L. Bjorno, J. Folsberg, and L. Pedersen, "Parametric arrays in shallow water," Journal De Physique, vol. 41, pp. 71-82, 1979 1979.
[7] J. R. Clynch and T. G. Muir, "Application of parametric arrays to shallow-water propagation," Journal of The Acoustical Society of America, vol. 57, pp. S64-S64, 1975 1975.
[8] F. J. Pompei, "The use of airborne ultrasonics for generating audible sound beams," Journal of The Audio Engineering Society, vol. 47, pp. 726-731, Sep 1999.
[9] M. Yoneyama, J.-i. Fujimoto, Y. Kawamo, and S. Sasabe, "The audio spotlight: An application of nonlinear interaction of sound waves to a new type of loudspeaker design," The Journal of the Acoustical Society of America, vol. 73, pp. 1532-1536, 1983.
[10] M. B. Bennett and D. T. Blackstock, "Parametric array in air," The Journal of the Acoustical Society of America, vol. 57, pp. 562-568, 1975.
[11] T. D. Kite, J. T. Post, and M. F. Hamilton, "Parametric array in air: Distortion reduction by preprocessing," The Journal of the Acoustical Society of America, vol. 103, pp. 2871-2871, 1998.
[12] Y. W. Kim and S. il Kim, "Novel preprocessing technique to improve harmonic distortion in airborne parametric array," 2002 6th International Conference on Signal Processing Proceedings, Vols I and Ii, pp. 1815-1818, 2002.
[13] Y. H. Liew, K. Lee, F. A. Karnapi, and W. S. Gan, "Using psycho-acoustics frequency masking to reduce distortion in a parametric array speaker," The Journal of the Acoustical Society of America, vol. 110, pp. 2741-2741, 2001.
[14] P. Ji, E.-L. Tan, and W.-S. Gan, "A Comparative Analysis of Preprocessing Methods for the Parametric Loudspeaker Based on the Khokhlov–Zabolotskaya–Kuznetsov Equation for Speech Reproduction," IEEE Transactions on Audio, Speech and Language Processing, vol. 19, pp. 937-946, 2011.
[15] I. O. Wygant, M. Kupnik, J. C. Windsor, W. M. Wright, M. S. Wochner, G. G. Yaralioglu, M. F. Hamilton, and B. T. Khuri-Yakub, "50 kHz capacitive micromachined ultrasonic transducers for generation of highly directional sound with parametric arrays " IEEE Transactions on Ultrasonics, Ferroelectrics and Frequency Control, vol. 56, pp. 193 - 203, 2009.
[16] I. O. Wygant, M. Kupnik, J. C. Windsor, W. M. Wright, M. S. Wochner, G. G. Yaralioglu, M. F. Hamilton, and B. T. Khuri-Yakub, "Capacitive micromachined ultrasonic transducers for generation of highly directional sound with a parametric array," The Journal of the Acoustical Society of America, vol. 123, pp. 3375-3375, 2008.
[17] Z. Wang, J. Miao, and W. Zhu, "Micromachined ultrasonic transducers and arrays based on piezoelectric thick film " Applied Physics A: Material Science and Processing, vol. 91, pp. 107-117, 2008.
[18] P. Muralt, N. Ledermann, J. Baborowski, B. A., S. Gentil, B. Belgacem, S. Petitgrand, A. Bosseboeuf, and N. Setter, "Piezoelectric micromachined ultrasonic transducers based on PZT thin films," IEEE

Transactions on Ultrasonics, Ferroelectrics and Frequency Control, vol. 52, pp. 2276-2288, 2005.
[19] R. O. Cleveland, M. F. Hamilton, and D. T. Blackstock, "Time-domain modeling of finite-amplitude sound in relaxing fluids," Journal of The Acoustical Society of America, vol. 99, pp. 3312-3318, Jun 1996.
[20] Y. S. Lee and M. F. Hamilton, "Time-domain modeling of pulsed finite-amplitude sound beams," Journal of The Acoustical Society of America, vol. 97, pp. 906-917, 1995.
[21] T. Christopher, "Finite amplitude distortion-based inhomogeneous pulse echo ultrasonic imaging," Ieee Transactions on Ultrasonics Ferroelectrics and Frequency Control, vol. 44, pp. 125-139, Jan 1997.
[22] "IEEE Standard on Piezoelectricity ANSI/IEEE Std 176-1987," IEEE Ultrasonics, Ferroelectrics, and Frequency Control Society, 1987.
[23] S. A. N. Prasad, Q. Gallas, S. Horowitz, B. Homeijer, B. V. Sankar, L. N. Cattafesta, and M. Sheplak, "Analytical Electroacoustic Model of a Piezoelectric Composite Circular Plate," AIAA Journal, vol. 44, pp. 2311-2318, 2006.
[24] E. Hong, S. Trolier-McKinstry, R. Smith, S. V. Krishnaswamy, and C. B. Freidhoff, "Vibration of micomachined circular piezoelectric diaphragms," IEEE Transactions on Ultrasonics, Ferroelectrics and Frequency Control, vol. 53, pp. 697-705, 2006.
[25] G. Anderson, "On the determination of finite integral transforms for forced vibrations of circular plates," Journal of Sound and Vibration, vol. 9, pp. 126-144, 1969.
[26] S. Kopuz, Y. S. Unlusoy, and M. Caliskan, "Integrated FEM/BEM approach to the dynamic and acoustic analysis of plate structures," Engineering Analysis with Boundary Elements, vol. 17, pp. 269-277, 1996.